

Alpha-2 Macroglobulin Controls Trophoblast Positioning in Mouse Implantation Sites

S. Esadeg^a, H. He^a, R. Pijnenborg^b, F. Van Leuven^c and B. A. Croy^{a,d}

^a Department of Biomedical Sciences, Ontario Veterinary College, University of Guelph, Building 40, Room 2604, Guelph, ON, Canada N1G 2W1; ^b Department of Obstetrics and Gynaecology, K.U. Leuven, B-3000 Leuven, Belgium; ^c Experimental Genetics Group, Department of Human Genetics, K.U. Leuven, B-3000 Leuven, Belgium

Paper accepted 3 June 2003

In humans, functional deficiency of α -2M is not known, implying α 2M is essential for gestational success. Mice, deficient in two members of the α -2 Macroglobulin (α 2M) family, i.e. α -2 macroglobulin (MAM) and murinoglobulin-1 (MUG-1) are viable, fertile and phenotypically normal, unless stressed (Am J Pathol, 155 (1999), 983). Here, we analysed implantation sites in MAM^{-/-}/MUG-1^{-/-} mice during pregnancy, a strong physiological stressor. Despite some post-implantation fetal loss, mean litter size was comparable to congenic C57Bl/6J (B6) mice, but MAM^{-/-}/MUG-1^{-/-} pups were significantly lighter and the sex ratio was skewed towards males. Implantation sites appeared histologically normal up to gestational day (gd) 8. By gd 10, extensive over-development of trophoblasts was evident, accompanied by relative deficits in decidua, in the mural mesometrial lymphoid aggregates of pregnancy and in uterine Natural Killer cells. At gd 10–12, decidual spiral arteries were dilated but abnormally cuffed by trophoblasts that extended anomalously, for midgestation, to the myometrial circular smooth muscle. Ultrastructurally, trophoblasts in the mesometrial decidua made intimate contact with endothelial cells that were shedding membrane fragments. These findings demonstrate that α 2M, and thereby proteinases and/or cytokines whose bio-availability is regulated by α 2M, exert significant decidual regulation on trophoblast invasion.

Placenta (2003), 24, 912–921

© 2003 Elsevier Ltd. All rights reserved.

INTRODUCTION

Alpha-2 macroglobulin (α 2M) is the major inhibitor of endo-proteinases and carrier of cytokines and growth factors in mammalian blood. Human α 2M, the best-studied member of the family, is a homo-tetramer of 180 kDa subunits (Sottrup-Jensen et al., 1984). α 2M has a unique mechanism of endo-proteinase binding or 'activation'. It involves (i) proteolytic cleavage of the bait-region, (ii) hydrolysis of the internal thiol-ester bonds and finally (iii) re-folding of α 2M around the proteinase, creating a physical 'trap' (Barrett and Starkey, 1973). This dramatic conformational change also exposes the receptor-binding domain allowing specific recognition and evacuation of α 2M-proteinase complexes by receptor-mediated endocytosis (for review see Van Leuven, 1982). Besides endo-proteinases, cytokines and growth factors bind to native and/or activated α 2M by simple association. The presumed roles of these interactions include (i) transport and (ii) clearance of cytokines, (iii) protection against toxic effects of cytokines, (iv) protection of the cytokine against degradation or renal clearance and (v) targeting of cytokines to cells expressing the α 2M-receptor (α 2M-R) or lipoprotein-receptor related protein (LRP) (LaMarre et al., 1991).

^d To whom correspondence should be addressed. Tel.: +1-519-824-4120x54915; Fax: +1-519-767-1450; E-mail: acroy@uoguelph.ca

In humans, uterine α 2M is thought to originate from endothelial cells lining the endometrial vessels and its concentration doubles or triples during the secretory relative to the proliferative phase of the menstrual cycle (Sayegh et al., 1997), a time coincident with recruitment of Natural Killer (NK) cells to human endometrium (Moffett-King, 2002). Pregnancy zone protein (PZP) is a second member of the human α 2M gene family. In normal plasma, PZP concentrations are practically undetectable, but concentrations rise to match or even exceed those of α 2M in plasma (2–4 mg/ml) in pregnant women. PZP is known to bind TGF- β 1 and - β 2 (Philip et al., 1994). In rats, α 2M is classified as an acute phase reactant and as a decidualization protein. Rat α 2M is not expressed by virgin endometrium but is highly expressed by midgestational mesometrial decidua under prolactin regulation (Thomas and Schreiber, 1989; Gu et al., 1992). Absence of α 2M expression in anti-mesometrial rat decidual cells is attributed to gene down regulation by the protein suppression of cytokine signalling-1 (SOCS-1), an inhibitor in the Jak/Stat signalling pathway (Barkai et al., 2000).

In mouse plasma, two major members of the α 2M family are characterized: the tetrameric mouse α 2M (MAM) and the monomeric murinoglobulin (MUG-1). Both proteins originate from the liver, the only organ expressing their mRNA (Lorent et al., 1994; Overbergh et al., 1995). Fetal expression of MAM

is also restricted to the liver and commences at gd 13. Postnatally, plasma concentrations of MAM are fairly constant (2–4 mg/ml), including during pregnancy. At least three genes coding for MUGs have been molecularly cloned (*MUG-1*, *MUG-2* and *MUG-3*) but only *MUG-1* appears to be effectively translated into a plasma protein (Overbergh, et al., 1994a). MUG-1 is not expressed during embryogenesis (Lorent et al., 1994) but appears in plasma after weaning and reaches adult concentrations 5–6 weeks later, with slightly higher levels in males than females (Overbergh et al., 1994b). During pregnancy, maternal hepatic MUG mRNA decreases significantly and is lowest between gd 10–16 (30 per cent of non-pregnant levels). Plasma MUG also drops from a pre-conception mean of 1 mg/ml to below 0.2 mg/ml at mid-gestation (Overbergh et al., 1995). MAM levels increase in the mouse uterus during gestation, likely due to increased permeability of uterine vessels to plasma proteins since no mRNA has been detected locally. This extravasation is observed during early pregnancy with highest concentrations of MAM at, rather than between, implantation sites (Bany and McRae, 1992). By microarray analysis of mRNA from mesometrial decidua at implantation sites in C57BL/6 (B6) mice at gd 6 and 10, we observed considerable increases in mRNA expression of MAM and of its receptor LRP. This suggested that in mouse, as in the rat, uterine stromal cells produce at least one member of the α 2M family and led to the current study evaluating the roles of MAM and MUG-1 in the circulation and/or from uterine origin on and at the implantation sites in B6 and MAM^{-/-}/MUG-1^{-/-} mice (Umans et al., 1999). We demonstrate that these molecules are important in limiting the rate of trophoblast invasion.

MATERIALS AND METHODS

Mice

MAM^{-/-}/MUG-1^{-/-} mice on the C57BL/6J genetic background ($N > 9$) (Umans et al., 1999) were housed and bred under barrier husbandry (OMAFRA Isolation Unit, University of Guelph) and wild-type C57BL/6J (B6) mice were purchased commercially (Jackson Labs, Bar Harbor, ME, USA). Some B6 mice were barrier housed, while most were maintained under conventional husbandry (Central Animal Facility, University of Guelph). All tests with animals were undertaken in accordance with the Guidelines for the Care and Use of Laboratory Animals (CCAC, Ottawa, Canada) and with protocols approved by the Animal Care Committee of the University of Guelph.

MAM^{-/-}/MUG-1^{-/-} pups appeared somewhat smaller than wild-type offspring and therefore weights were obtained at 4, 6 and 8 weeks of age. At 10 weeks of age, oestrous females were paired with syngeneic males overnight and vaginal plug detection in the morning was defined as day 0 of pregnancy. Age and gd-matched wild-type B6 pregnant mice were used as controls. Pregnant mice were euthanized by CO₂ followed by

cervical dislocation. At least three implantation sites from each of three females were studied at gd 6, 8, 10 and 12. Implantation sites from two females were available at days 11, 13, 14, 15 and 16.

RT-PCR

RT-PCR was conducted on cDNA prepared from total RNA isolated from 20 dissected tissues from virgin, gd 10 pregnant, and multiparous but non-pregnant wild-type B6 mice and from testis of a proven stud male. Primers specific for the 'signature'-bait regions were for MAM: 5'-CCTGTCAACAGCATCCAAGA and 5'-GATCCTGACCCTTTGGTGAC yielding an amplicon of 276 bp and for MUG-1: 5'-GTTTTGACTTGGCATGGTT and 5'-GCACACTCATCTGCATGCTT producing an amplicon of 447 bp. Mouse β -Actin (β -Act) was used as the internal RT-PCR control using primers 5'-GCTACAGCTTCACCACCACA and 5'-ACATCGCTGGAAGGTGGAC (amplicon of 477 bp). The PCR conditions were: 94°C 6 min; 30 cycles of 94°C 30 sec, 56°C 60 sec, 72°C 60 sec, followed by 7 min at 72°C and final storage at 4°C. Products were run on 1 per cent agarose gels, stained with ethidium bromide and imaged using standard techniques.

Tissue fixation, embedding and staining

Following euthanasia, mice were opened mid-ventrally, the heart was exposed and 15 ml of freshly prepared 4 per cent paraformaldehyde in 0.1 M sucrose (PFA) were perfused into the dorsal aorta or uterine arteries slowly over a 15 min interval. The right atrium was incised after the first 2–3 min to provide drainage. Skin, kidney and uteri were then dissected and processed for histology. Fixed uteri were examined grossly for number and viability of implants (based on large size and pink colour), dissected into individual implant sites and immersed in 4 per cent PFA, for 1 h (specimens up to and including gd 10) or 6 h (specimens gd 11+) for further fixation. Specimens were then washed in PBS (15 min), and processed into wax blocks automatically (1530 Paraffin Tissue Processor, RMC, Tucson, Arizona, USA) and prepared as 7 μ m thick transverse serial sections.

For general histology, sections were stained with Haematoxylin and Eosin (H&E). For identification of uNK cells, Periodic Acid-Schiff's reagent (PAS) or *Dolichos biflorus* agglutinin lectin (DBA; Sigma-Aldrich, Oakville, ON, Canada), was used to reveal cytoplasmic granulation (Peel, 1989; Paffaro et al., 2003). DBA also reacts with uNK cell plasma membranes and was used to include immature, non-granulated uNK cells among counted cells (Stewart and Webster, 1997; Paffaro et al., 2003).

Immunohistochemistry

Immunohistochemistry was conducted on selected sections using rabbit anti-bovine pancytokeratin (Dako, Mississauga,

ON, Canada; Z0622, 1 : 1000) to localize trophoblast cells. Sections were incubated in proteinase K (Dako; 5 min; 20°C), washed in 0.1 M PBS, incubated in 3 per cent H₂O₂ (30 min), washed in PBS and incubated in universal block solution (CD310082, Dako; 30 min). Primary antibody or non-immune rabbit serum was applied to all sections (4°C, overnight). Mouse skin and kidney were used as positive tissue controls. After two rinses, the EnVision system (DAKO K1491) was used, according to manufacturer's instructions. Diaminobenzidine (DAB) was used as the chromagen and sections were counterstained using Harris's haematoxylin.

Enumeration of NK and decidual cells and morphometric analyses of implantation sites

All serial sections were examined to obtain information on each implantation site. Eleven sections from the middle of each implantation site were analysed in detail using a 1 mm² ocular grid at 500× magnification. The central location of the selected sections was confirmed by entry of uterine artery branches. To avoid duplicate counting of uNK cells, which can exceed 40 µm in diameter, the sections analysed in detail were 42 µm apart. Myometrial circular smooth muscle was used as the boundary demarcating the mesometrial lymphoid aggregate of pregnancy (MLAp) from the decida basalis (DB). Area morphometry of MLAp, DB and placenta (delimited by giant cells) was conducted on the same 11 sections per implantation site. Line morphometry was performed to obtain cross sectional wall (W) and lumen (L) diameters of the decida spiral arteries using OPTIMAS image analysis software, version 6.2 (Optimas Corporation, Bothwell, MA, USA). Multiple implantation sites from at least three dams were studied for each data set presented.

Transmission electron microscopy

Mesometrial tissues (DB, MLAp and placenta (PL)) from gd 10 and 11 MAM^{-/-}/MUG-1^{-/-} and C57BL/6J mice were finely minced (1 mm³) and placed ice-cold fresh fixative (2.0 per cent glutaraldehyde and 2.5 per cent paraformaldehyde in 0.1 M phosphate buffer, pH 7.4) for 4 h. Tissues were post-fixed 1 h in 2 per cent osmic acid in 0.1 M phosphate buffer and routinely processed into Epon resin. Areas of interest were selected from semi-thin sections (1 µm) stained with toluidine blue. Ultra-thin sections, approximately 80 nm in thickness, were cut using Sorvall-MT-2B microtome (Dupont Instruments, Newtown, CT, USA), transferred to clean, coated-copper grids, contrasted with uranyl acetate and lead citrate and viewed on a JEOL-100S transmission electron microscope (TEM).

Statistical analyses

One-way analysis of variance (ANOVA) was used to test means between experimental groups. Tukey's test was used to

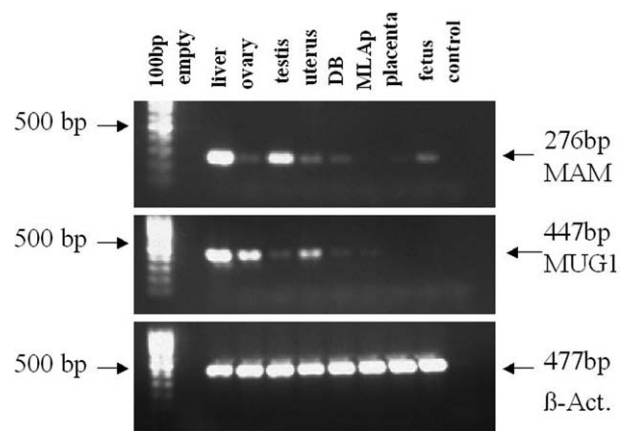


Figure 1. Ethidium bromide stained gels following electrophoresis of RT-PCR products for MAM, MUG-1 and β actin. Lane 1: 100 bp marker ladder; lane 2 no sample; lane 3: adult liver; lane 4: adult, non pregnant ovary; lane 5: testis; lane 6: virgin uterus; lane 7: gd 10 DB; lane 8: gd 10 MLAp; lane 9: gd 10 placenta (trophoblast portion); lane 10: gd 10 fetus; lane 11: water amplification control.

establish significant differences between groups. $P < 0.05$ was considered a significant difference.

RESULTS

Expression of MAM and MUG-1 in reproductive tissues

MAM and MUG-1 expression in the reproductive tract was examined by RT-PCR in B6 wild-type mice; livers from the same animals were used as controls (Figure 1 and not shown). MAM mRNA was expressed in liver of adult mice (virgin, gd 10 pregnant and non-pregnant multiparous females) and gd 10 fetuses. MAM and MUG-1 were also expressed in the ovaries of virgin, gd 10 and nonpregnant-multiparous B6 females as well as in B6 testes. MAM expression was detected in non pregnant uterus and in gd 10 DB but not in MLAp or PL (trophoblasts). MUG-1 mRNA had a comparable pattern but with indications for quantitative differences except that MUG-1 was not expressed in gd 10 fetal liver (Figure 1, Lane 10). Adult female brain, lymph nodes, lung, spleen, and bone marrow were all devoid of expression of MAM and of MUG-1 mRNA under all of the reproductive states examined.

Pregnancy in MAM^{-/-}/MUG-1^{-/-} mice

MAM^{-/-}/MUG-1^{-/-} mice (10 pairs and 32 litters analysed) produced somewhat smaller litters (4.9 ± 2.3 pups) compared to the published mean litter size of 7.0 (Technical data sheets, Jackson Laboratory, Bar Harbor, ME, USA) or to either of our colonies of B6 mice [6.1 ± 2.4 pups (4 pairs, 10 litters analysed in the conventional colony) and 7.6 ± 3.8 pups (4 pairs, 12 litters analysed in the barrier-husbandry colony)]. Although these differences were not statistically significant, we

Table 1. Fetal survival in pregnant MAM^{-/-}/MUG-1^{-/-} mice and in congenic B6 controls.

Day of Gestation	MAM ^{-/-} /MUG-1 ^{-/-}			C57B1/6J		
	# of Dams	# of viable/total implants	% viability	# of Dams	# of viable/total implants	% viability
6	2	16/17	94.1	2	11/11	100
8	2	11/16	68.8	3	18/18	100
10	4	30/37	81.1	4	32/33	96.9
12	7	49/56	87.5	8	56/60	93.3

observed MAM^{-/-}/MUG-1^{-/-} resorption sites at mid-gestation indicating that these fetuses were less viable than B6 fetuses (Table 1). Any implantation sites with suspected fetal death were excluded from histological analysis.

Among live-born, the male:female ratio was 2:1 for MAM^{-/-}/MUG-1^{-/-} neonates and all offspring were smaller than those produced by B6 parents. Even in adults, average weights of female and male MAM^{-/-}/MUG-1^{-/-} mice were less than sex- and age-matched B6 controls raised in our colony (results not shown) and as reported in the supplier's colony. At age 4, 6 and 8 weeks, mean weights of female MAM^{-/-}/MUG-1^{-/-} were 11.1, 14.9 and 17.5 g respectively, compared to 14.3, 18.4 and 19.0 g for B6 females. Mean weights of male MAM^{-/-}/MUG-1^{-/-} at 4, 6 and 8 weeks were 12.7, 18.5 and 22.5 g compared to 17.1, 22.8 and 25.2 g for B6 males, respectively. For this reason, the weaning and mating of MAM^{-/-}/MUG-1^{-/-} was delayed by 2 weeks, relative to congenic B6 controls.

Implantation site morphology in MAM^{-/-}/MUG-1^{-/-} mice

Implantation site morphology gd 6–10. At gd 6 and gd 8, implantation sites in MAM^{-/-}/MUG-1^{-/-} mice appeared normal and histologically similar to those in B6 mice (not shown). By gd 10 (Figure 2), the DB in MAM^{-/-}/MUG-1^{-/-} mice appeared hypocellular although it occupied an area equal to that in B6 mice (summarized in Figure 3C). MAM^{-/-}/MUG-1^{-/-} decidual cells contained smaller nuclei and they were smaller cells (hypotrophic) than B6 decidual cells. Inter-cellular space between MAM^{-/-}/MUG-1^{-/-} decidual cells was increased (Figure 2C). UNK cell frequency per unit area of DB was significantly less in MAM^{-/-}/MUG-1^{-/-} than in B6 mice (Figure 3D). The MLAp developed and at gd 10 was approximately normal in area to B6 and had normal frequency of uNK cells (not shown). The decidua/trophoblast interface was highly anomalous (Figure 2A, B) compared to that in B6 mice (Figure 2D). The typical dome of giant cells was extensively disrupted by compact tissue comprised of large mono- and bi-nuclear eosinophilic cells which extended deeply into DB, almost reaching the circular smooth muscle. This anomaly is

presented as a diagram in Figure 2B. The unusual tissue surrounded the spiral arteries (Figure 2E compared to F) but was not included in the morphometric measurements of spiral artery wall thickness unless adjacent to an endothelial cell. The spiral arteries of MAM^{-/-}/MUG-1^{-/-} appeared dilated and this was confirmed by measurements showing wall:lumen ratios for MAM^{-/-}/MUG-1^{-/-} were not statistically different from the ratios for the same vessels found in the dilated state at gd 10 in normal mice (data not shown; Guimond et al., 1997; Ashkar, Di Santo and Croy, 2000).

Implantation site morphology gd 12–16. MAM^{-/-}/MUG-1^{-/-} implantation sites in the second half of gestation retained the distinctive features seen at gd 10 and displayed additional differences to the control implantation sites (Figure 3A, B). The DB remained equal in size to that of B6 but had fewer uNK cells (Figure 3C, D) The MLAp area was statistically smaller than in matched controls but uNK cell density matched that of B6, yielding a relative uNK cell deficit. Placentae in MAM^{-/-}/MUG-1^{-/-} mice were significantly larger than in B6 mice ($P < 0.05$; Figure 3C) and, after mid-gestation, it could be appreciated that there was limited development of the labyrinthine zone (Figure 3A compared to B). At gd 15 and 16, further placental growth was evident. The decidual spiral arteries were widely dilated but remained wrapped by large cells that were now present as much narrower cuffs (Figure 3B). Dilated, distal components of the spiral arteries, in the MLAp between the myometrial circular and longitudinal smooth muscle layers, were not cuffed by this type of cell.

Trophoblast overgrowth in the decidua basalis of mid-gestation MAM^{-/-}/MUG-1^{-/-} mice

Cytokeratin immunocytochemistry was performed on gd 10–15 implantation sites to identify the large, mono- and bi-nucleate, spiral artery-associated cells. They were shown to be cytokeratin reactive, suggesting the trophoblast lineage (Figure 4). In MAM^{-/-}/MUG-1^{-/-} mice, these trophoblasts were embedded in spiral artery walls and surrounded the entire vessel circumference (Figure 4A insert, D). At gd 10–12, these perivascular and intramural trophoblast cells extended to

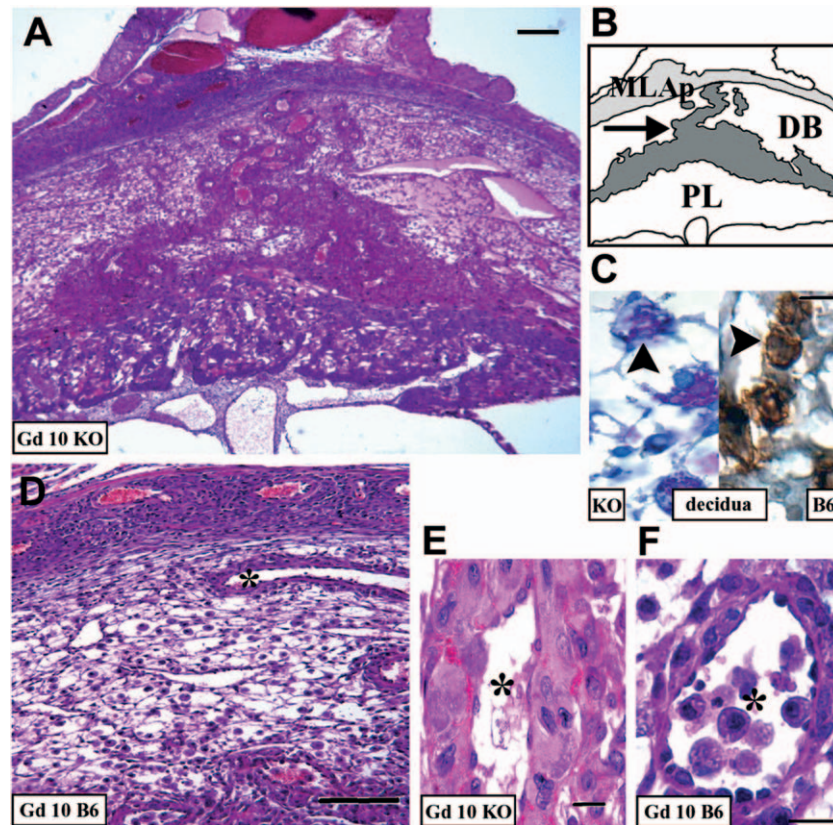


Figure 2. Mesometrial aspects of implantation sites at gd 10 in $MAM^{-/-}/MUG-1^{-/-}$ (KO; A, C-left side, E and diagrammed in B) and B6 (C-right side, D, F). In all images, the placenta is depicted towards the bottom of the image and MLAp towards the top. (A) shows the presence of an unusual cone of darkly stained, densely packed cells in the decidua basalis that extends along the full length of the spiral arteries to the circular smooth muscle layer. These cells were observed in all gd 10 $MAM^{-/-}/MUG-1^{-/-}$ but were not seen at gd 10 in normal mice (D). (A) and (D) stained with H&E. Bar represents 200 μ m. (B) is a diagram depicting the key microdomains in mouse implantation sites at mid gestation. The stippled region is the anomalous feature found in $MAM^{-/-}/MUG-1^{-/-}$ but absent from B6 controls. The placental region marked PL was delimited by giant cells which were used as the boundary for the morphometric measurements of placental tissue area (i.e. the stippled region was not included). (C) contrasts the decidua basalis in $MAM^{-/-}/MUG-1^{-/-}$ (on left, PAS stained to identify 2 uNK cells) to B6 (on right, DBA lectin stained to identify 6 uNK cells) and illustrates the large intercellular spaces and lack of decidual structural detail in the gene-ablated mice. Bar represents 50 μ m. (E) depicts, at higher magnification, the unusual cell population cuffing the spiral arteries and embedded in their walls. No equivalent cells were present in this region in gd-matched normal B6 controls (F). H&E stained, bar represent 10 μ m in (E) and 20 μ m in (F). * represents lumen of a cross-sectional spiral artery.

the circular smooth muscle but did not cross it. Trophoblast in gd-matched B6 mice does not display this depth of invasion (compare Figure 4A to B), until gd 18 (not shown). The endothelial lining of the invaded arteries appeared to be maintained by light microscopy (Figure 4A insert and 4D) and intravascular uNK cells were observed. No cytokeratin-positive cells were detected in the MLAp or the uterine wall at mid or late pregnancy.

Ultrastructure of the decidua, spiral arteries and placentae of $MAM^{-/-}/MUG-1^{-/-}$ mice

At gd 10 and 11, the increased intercellular spaces observed in paraffin sections of DB from $MAM^{-/-}/MUG-1^{-/-}$ mice were prominent ultrastructurally. Fewer stromal cells contacted uNK cells (Figure 5A compared with 5B). Many uNK cells appeared normal with structurally intact granules and

other organelles but other uNK cells showed evidence of early degenerative changes including nuclear chromatin margination and mitochondrial swelling. These degenerative changes are typical in wild-type mice after gd 12 (Peel, 1989; Paffaro et al., 2003).

Large, irregular mono- and bi-nucleate trophoblast-like cells with abundant endoplasmic reticulum and small mitochondria were seen in the walls of spiral arteries (Figure 5C, D). The endothelial lining of the spiral arteries was maintained but many endothelial cells appeared desquamated or showed cytoplasmic blebbing and degeneration (Figure 5C–F). Cytoplasmic processes of some trophoblast-like cells appeared to separate the basement membrane support of the endothelium (Figure 5D).

Ultrastructural examination of the placental labyrinthine showed that the cytoplasm of $MAM^{-/-}/MUG-1^{-/-}$ trophoblast cells contained more phagolysosomes and lamellar bodies than B6 trophoblasts (Figure 6) where they contributed to haemotrichorial membranes.

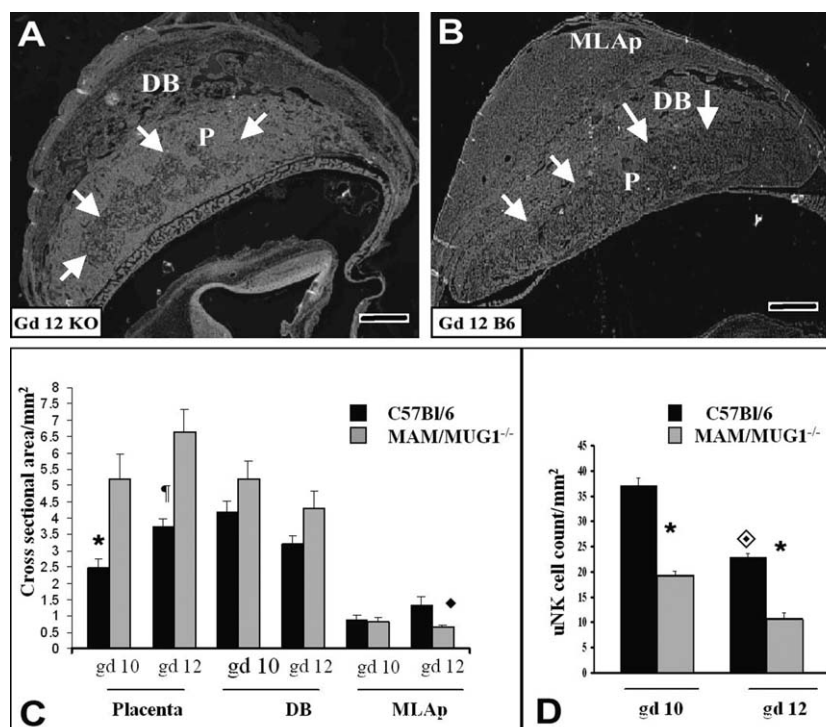


Figure 3. The mesometrial aspects of H&E-stained implantation sites viewed under dark field from gd 12 in MAM^{-/-}/MUG-1^{-/-} (KO; A) and B6 (B) mice and summary of morphometric analyses of subdomain cross sectional areas and uNK cell numbers in MAM^{-/-}/MUG-1^{-/-} and B6 at gd 10 and 12. The features seen at gd 10 were retained as the placentae grew to gd 16. The large eosinophilic cells that cuffed dilated spiral arteries to the circular smooth muscle layer remained present (not shown). MAM^{-/-}/MUG-1^{-/-} placentae (P) were disproportionately large to decidua basalis. The labyrinthine zone (marked by white arrows) was smaller than in the normal control (B) and showed a pattern of irregular constrictions that were associated with vascular channels (arrowtips in A). Magnification bars are 400 μ m. Areas occupied by placental tissue in MAM^{-/-}/MUG-1^{-/-} sections were nearly double those of B6 on both days analysed and statistically different (*, \ddagger respectively; C). Decidua basalis was similar in area, as a region, for the two strains although MAM^{-/-}/MUG-1^{-/-} decidual cells were hypotrophic. The MLAp area was significantly smaller only at gd 12 (\blacklozenge). Frequency of uNK cells in decidua basalis at gd 10 and 12 is shown in (D). Fewer uNK cells were present in the gene-ablated mice than B6 in this tissue microdomain (* P <0.05). Each strain had lower numbers of uNK cells at gd 12 than at gd 10 in that strain (\blacklozenge), indicating a normal decline in this cell population as previously reported by us and others (Peel, 1989).

DISCUSSION

Circulating α 2M in humans, MAM in mice and their associated family members are not only endoproteinase inhibitors but also major regulatory molecules that control functional availability of cytokines, hormones and growth factors (Bhattacharjee et al., 2000). Members of this gene family have been associated with fronts of tissue remodeling (Gu et al., 1992). During pregnancy, substantial and complex tissue remodeling is essential for implantation site development and an extended cytokine network is activated within the uterus, with various extensions into the entire female body (Sacks et al., 1998). Both leukocytic and non-leukocytic cells produce an array of cytokines that need to be tightly regulated to avoid pathological sequelae, such as pre-eclampsia and spontaneous abortion (Conrad and Benyo, 1997; Carp et al., 2001). The present study contributes to functional definition of cytokine control mechanisms. It demonstrates that in addition to the peri-implantation extravasation of MAM and probably of MUG-1 at lower concentrations, post-implantation expression of MAM (but not MUG-1) occurs within the uteri of pregnant wild-type mice. The combined functions of extravasated and uterine synthesized MAM are clearly to limit the rate of

trophoblast invasion. In MAM^{-/-}/MUG-1^{-/-} mice, trophoblasts, at mid-gestation, had already reached a position similar to that in very late gestation (17.5 days) wild-type mice.

Spiral arteries in MAM^{-/-}/MUG-1^{-/-} mice were fully dilated by gd 10. This may result from a reduced but adequate function of uNK cells (Ashkar, Di Santo and Croy, 2000) or be due, at least in part, to changes induced by the unusual perivascular trophoblasts. The encircling trophoblasts did not reach the lumens of the arteries, a key difference between the analogous vessels in mouse and human. In wild-type mice, even in late gestation, intravascular trophoblasts remain within 150–300 μ m of the giant cell layer (Adamson et al., 2002; Cross et al., 2002) while intramural trophoblasts extend to the circular smooth muscle (personal observations). The multinucleate feature, general appearance and location of the unusual trophoblast cells suggest they most probably derive from spongiotrophoblast and maybe differentiating towards giant cells. This could be confirmed by in situ localization of specific transcription factors (Cross et al., 2002). We observed that many of the endothelial cells overlying the intramural trophoblast in MAM^{-/-}/MUG-1^{-/-} mice were degenerating, but it is not clear whether degeneration preceded or followed the time-point when trophoblasts assumed their unusual position.

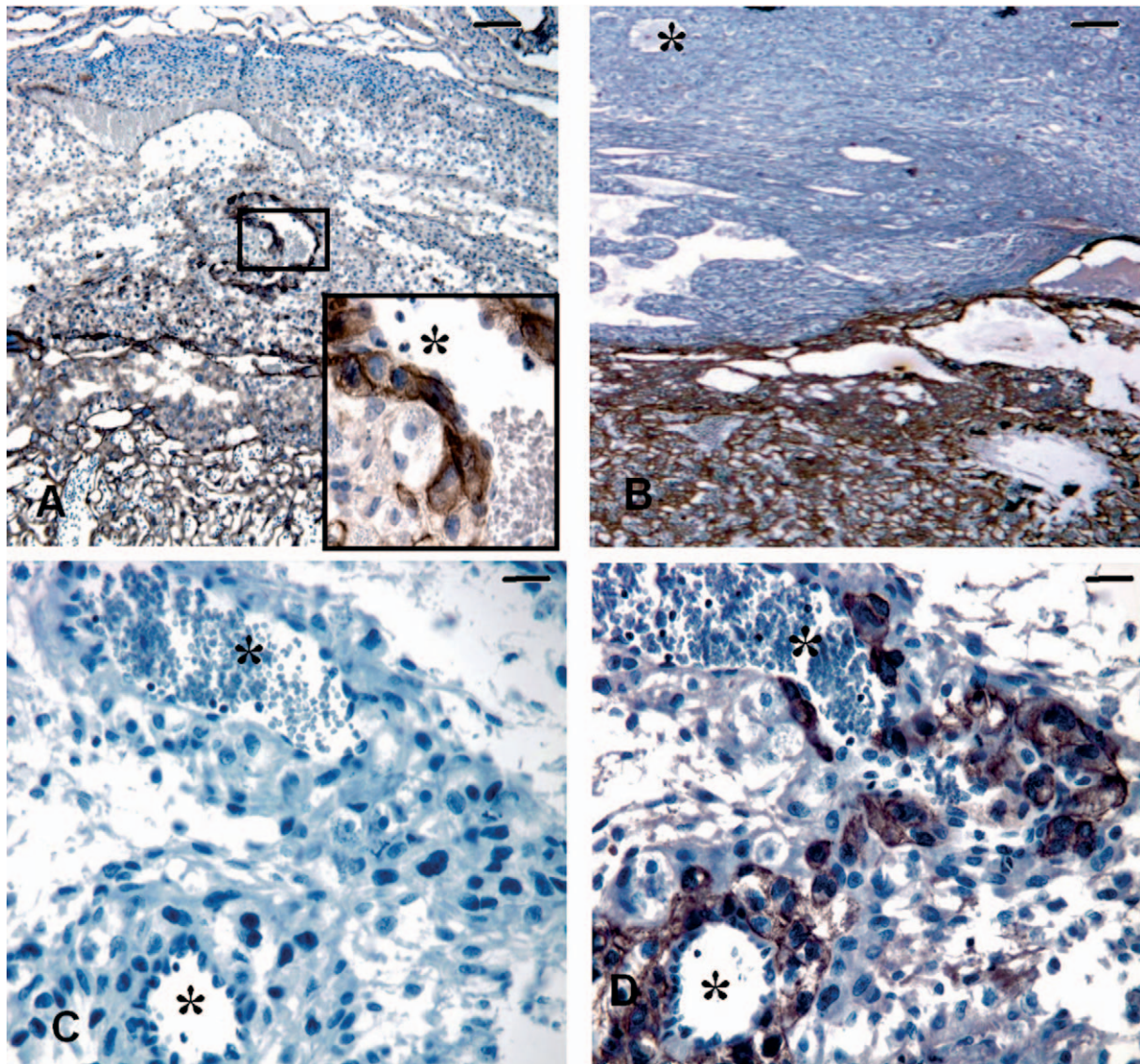


Figure 4. Photomicrographs of immunohistochemistry for cytokeratin (A, B and D) used for the identification of trophoblast lineage cells and the normal rabbit serum control (C) on gd 11 $MAM^{-/-}/MUG-1^{-/-}$ (A, C, D) and B6 (B) implantation sites. Cytokeratin reactive cells with the morphology of large trophoblast cells (insert in A) cuffed the larger vessels in the decidua basalis of $MAM^{-/-}/MUG-1^{-/-}$ but not B6. (D) compared to (C) shows cytokeratin reactive cells in semi-adjacent sections fully surrounding a vessel. Trophoblast cells remained intramural (extraluminal) and were always covered by endothelial cells (A insert and D). Bars in A and B are 200 μm . Bars in C and D are 50 μm . * represents lumen of a cross-sectioned spiral artery.

Since a deficit in proteinase inhibition must occur in the absence of MAM and MUG-1, endothelial cells in the gene-deficient mice would be constantly stressed, as reflected in their ultrastructure. This hypothesis becomes highly plausible considering the high level of $\alpha 2\text{M}$ in human uterine endothelial cells (Sayegh et al., 1997) and trophoblast recruitment might be a subsequent repair response. Besides proteinase activity, a deficit in growth factors having positive effects on endothelial cells must be considered in the null mice, because the normal control mechanisms exerted by the many and diverse signalling molecules that bind to $\alpha 2\text{M}$ will be disrupted.

Alternatively, deficient proteinase blocking in DB may passively allow trophoblast invasion to proceed unopposed. A

major function of decidua, frequently proposed by others, is to limit invasion of trophoblast. Our study identifies MAM as a key mechanism whereby decidual cells indeed regulate trophoblast cell invasion. Work with human trophoblast cell lines in vitro found that $\text{TGF-}\beta$ was a negative regulator of trophoblast invasion (Graham, 1997). Because $\text{TGF-}\beta$ binds to all naturally occurring forms of $\alpha 2\text{M}$, it is possible that in vivo, the complex of $\alpha 2\text{M}$ and $\text{TGF-}\beta$ is the most potent negative regulator of trophoblast position within DB. MAM is not the only molecule regulating mesometrial trophoblast invasion. Although trophoblasts in $MAM^{-/-}/MUG-1^{-/-}$ reached the circular smooth muscle by gd 10, they did not cross it even in late gestation, suggesting that myometrium and MLAp represent distinct functional microdomains retaining

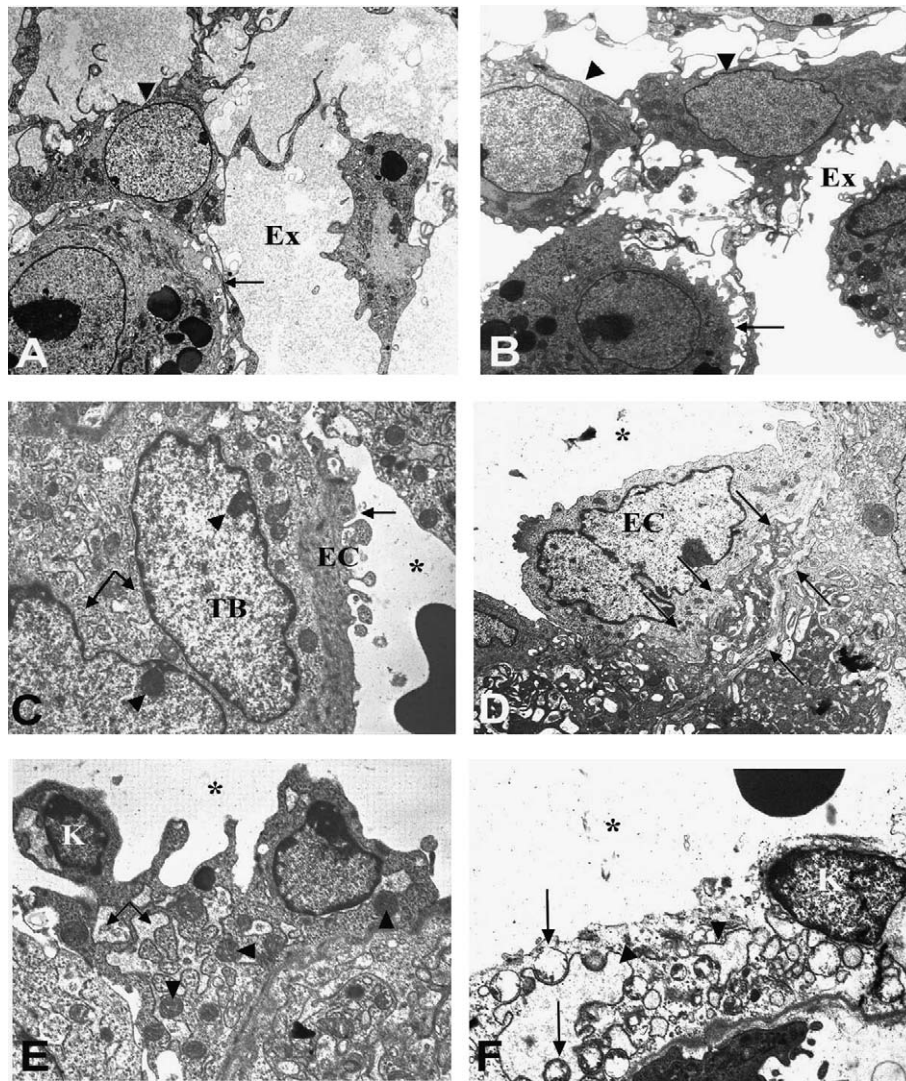


Figure 5. Ultrastructural images from gd 11 DB of $MAM^{-/-}/MUG-1^{-/-}$ (A; C–F) and B6 (B) mice. Healthy uNK cells are compared (arrows) in the bottom of images (A and B; $\times 3000$). uNK cells are recognized by their membrane-bound cytoplasmic granules and eccentric nuclei. Decidual cells (arrowheads) in $MAM^{-/-}/MUG-1^{-/-}$ were hypotrophic (A) had displayed less cytoplasm and more prominent cytoplasmic processes than in B6 (B). Extracellular space (Ex) was much larger between decidual cells in the mutant mice. (C to F) depict the range of cell morphologies seen in the walls of the spiral arteries. (C) depicts a large binucleate cell (double-headed arrow) with the morphology of trophoblast (TB). Nucleolar margination, indicating protein synthesis, is indicated by arrowheads. The lumen of the artery is indicated as * and a mature erythrocyte is located within the vessel (lower right). The endothelial cell (EC) overlying the trophoblast shows cytoplasmic blebbing (arrow) $\times 3000$. (D) shows a portion of a trophoblast-like cell (arrows) separating an endothelial cell from its basal lamina. This event would precede endothelial cell detachment, which was also observed (not shown) $\times 4000$. (E) shows a degenerating endothelial cell with condensed mitochondria (arrowheads), swollen rough endoplasmic reticulum (arrows) and a pyknotic, extruding nucleus (K) $\times 6000$ while (F) depicts another dying endothelial cell with nuclear pyknosis (K), and numerous swollen organelles (arrows indicate swollen mitochondria; arrowheads indicate swollen rough endoplasmic reticulum $\times 6000$).

the ability to repel or lacking signals to recruit trophoblasts. That MAM mRNA was not detectably expressed in the MLAp of wild-type mice supports the uniqueness of this transient structure compared to DB.

The unusual position of trophoblast cells in $MAM^{-/-}/MUG-1^{-/-}$ mice was not the only difference found in comparison to wild-type mice (Georgiades, Ferguson-Smith and Burton, 2002). Within the placenta, trophoblast cells showed greater abundance of cytoplasmic organelles, including lipid droplets, which suggested metabolic stress on these cells

and a functional deficiency. The small size of $MAM^{-/-}/MUG-1^{-/-}$ pups also suggests placental insufficiency, despite larger than normal placentae in $MAM^{-/-}/MUG-1^{-/-}$. Two other strains of mice are reported with decidual compromise and placental overgrowth, IGF-BP1 transgenic mice (Crossey, Pillai and Miell, 2002) and p57Kip-2 null mice (Kanayama et al., 2002) but the features of both are distinct from $MAM^{-/-}/MUG-1^{-/-}$ mice. Over expression of human IGFBP-1 resulted in labyrinthine zone overdevelopment, while placentae of p57Kip-2 null mice

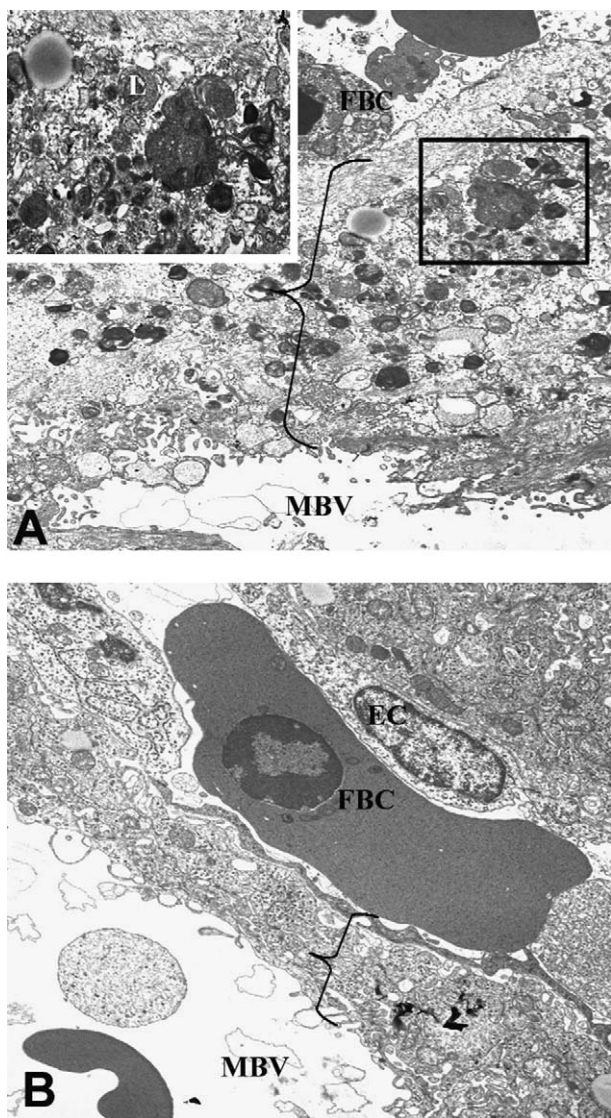


Figure 6. Ultrastructure of the placental haemotrichorial interface (bracket) at gd 11 in $MAM^{-/-}/MUG-1^{-/-}$ (A) and B6 (B). Numerous secondary lysosomes of different sizes and stages were evident in the placenta of $MAM^{-/-}/MUG-1^{-/-}$ mice (inset in A $\times 8000$) as compared to B6 control (B). L, lipid droplet; FBC, RBC within fetal blood vessel; MBV, maternal blood vessel and EC, endothelial cell. A ($\times 3000$) and B ($\times 4000$).

show spongiotrophoblast over-development. $MAM^{-/-}/MUG-1^{-/-}$ mice have underdevelopment of the labyrinth and over-development with vessel-associated trophoblast, which is most probably giant cell lineage. In all three strains, the DB is relatively deficient in area; its structural abnormality demonstrated here by TEM in $MAM^{-/-}/MUG-1^{-/-}$ mice. The ultrastructural damage to endothelial cells documented in

the spiral arteries (Figure 5C–F) could permit vascular leakage and tissue oedema that would be reflected as ultrastructural openness between cells (Figure 5A). Furthermore, the known role of $\alpha 2M$ s in the functional regulation of TGF- β , a key component of extracellular and perivascular matrices, suggests that matrix deficits are likely to limit vigorous transformation of endometrial stromal cells into decidual cells. Both IGF-BP1 over-expressing mice and p57Kip-2 null mice have been proposed as murine models of pre-eclampsia based on proteinuria, hypertension and other clinical features, but assessment of their spiral artery modification is not yet reported. Clinical assessments of pregnant $MAM^{-/-}/MUG-1^{-/-}$ mice are yet to be conducted but our demonstration of spiral artery dilation suggests these mice will be more important models for regulatory studies of trophoblast invasion than for studies of gestational hypertension. Other anomalies identified in implantation sites of pregnant $MAM^{-/-}/MUG-1^{-/-}$ mice are the reduced size of MLAp at gd 12, the reduction in number and maturity of decidual uNK cells and premature uNK cell degeneration at gd 10–12. Uterine NK cells produce a variety of cytokines, i.e. TNF- α (Yelavarthi et al., 1991), TGF- β (Tamada et al., 1990), IFN- γ (Ashkar, Di Santo and Croy, 2000) that regulate cell proliferation and bind to $\alpha 2M$. De-regulation of cytokine availability likely contributes to the aberrations in uNK cells.

$MAM^{-/-}/MUG-1^{-/-}$ mice were originally reported to produce normal sized litters (Umans et al., 1999). The current mid-pregnancy studies indicate a substantial gestational loss (~ 39 per cent) that greatly exceeds those in IGF-BP1 transgenic females (Crossey, Pillai and Miell, 2002). Furthermore, both male and female $MAM^{-/-}/MUG-1^{-/-}$ pups weighed less than congenic normal mice and maintained lower weights into adulthood. These findings suggest that this dual knockout strain has great potential and importance for the evaluation of the Barker hypothesis on fetal programming (Barker, 1999). We have yet no explanation for the skewed sex ratio, but our data showing expression of MAM and MUG-1 in the testes, corroborating previous reports (Braghiroli et al., 1998) suggest that the basis for the observed skewed distribution could arise within the male gonad.

Rises in plasma concentrations of PZP and, to a lesser extent $\alpha 2M$, during human pregnancy are long known (Ganrot and Bjerre, 1967) but remain unexplained. If these molecules are present within human implantation sites, they will contribute to regulation of the rate of trophoblast invasion. Our observations strongly suggest that there is merit in further investigation in experimental systems and in humans of the role of the $\alpha 2M$ gene family members and their functions in implantation and pregnancy.

ACKNOWLEDGEMENTS

These studies were supported by awards from the Natural Sciences and Engineering Council, of Canada and the Ontario Ministry of Agriculture, Food and Rural Affairs, and from Fonds voor Wetenschappelijk Onderzoek-Vlaanderen (FWO-Vlaanderen). We thank Drs M. A. Hayes, S. Yamashiro and O. Atwal for helpful discussions, Mary Ellen Junkins for assistance with the illustrations and the staff of the OMAFRA Animal Isolation Unit for their dedicated care of our barrier-reared mice.

REFERENCES

- Adamson SL, Lu Y, Whiteley KJ, Holmyard D, Hemberger M, Pfarrer C & Cross JC (2002) Interactions between trophoblast cells and the maternal and fetal circulation in the mouse placenta. *Dev Biol*, **250**, 358–373.
- Ashkar AA, Di Santo JP & Croy BA (2000) Interferon gamma contributes to initiation of uterine vascular modification, decidual integrity, and uterine natural killer cell maturation during normal murine pregnancy. *J Exp Med*, **192**, 259–270.
- Bany BM & McRae AC (1992) Uterine uptake of alpha 2-macroglobulin and alpha 1-proteinase inhibitor from the blood during early implantation in the mouse. *Biol Reprod*, **47**, 514–519.
- Barkai U, Prigent-Tessier A, Tessier C, Gibori GB & Gibori G (2000) Involvement of SOCS-1, the suppressor of cytokine signaling, in the prevention of prolactin-responsive gene expression in decidual cells. *Mol Endocrinol*, **14**, 554–563.
- Barker DJ (1999) The long-term outcome of retarded fetal growth. *Schweiz Med Wochenschr*, **129**, 189–196.
- Barrett AJ & Starkey PM (1973) The interaction of alpha 2-macroglobulin with proteinases. Characteristics and specificity of the reaction, and a hypothesis concerning its molecular mechanism. *Biochem J*, **133**, 709–724.
- Bhattacharjee G, Asplin IR, Wu SM, Gawdi G & Pizzo SV (2000) The conformation-dependent interaction of alpha 2-macroglobulin with vascular endothelial growth factor. A novel mechanism of alpha 2-macroglobulin/growth factor binding. *J Biol Chem*, **275**, 26806–26811.
- Braghiroli L, Silvestrini B, Sorrentino C, Grima J, Mruk D & Cheng CY (1998) Regulation of alpha2-macroglobulin expression in rat Sertoli cells and hepatocytes by germ cells in vitro. *Biol Reprod*, **59**, 111–123.
- Carp H, Torchinsky A, Fein A & Toder V (2001) Hormones, cytokines and fetal anomalies in habitual abortion. *Gynecol Endocrinol*, **15**, 472–482.
- Conrad KP & Benyo DF (1997) Placental cytokines and the pathogenesis of preeclampsia. *Am J Reprod Immunol*, **37**, 240–249.
- Cross JC, Hemberger M, Lu Y, Nozaki T, Whiteley K, Masutani M & Adamson SL (2002) Trophoblast functions, angiogenesis and remodeling of the maternal vasculature in the placenta. *Mol Cell Endocrinol*, **187**, 207–212.
- Crossey PA, Pillai CC & Miell JP (2002) Altered placental development and intrauterine growth restriction in IGF binding protein-1 transgenic mice. *J Clin Invest*, **110**, 411–418.
- Ganrot PO & Bjerre B (1967) Alpha-1-antitrypsin and alpha-2-macroglobulin concentration in serum during pregnancy. *Acta Obstet Gynecol Scand*, **46**, 126–137.
- Georgiades P, Ferguson-Smith AC & Burton GJ (2002) Comparative developmental anatomy of the murine and human definitive placentae. *Placenta*, **23**, 3–19.
- Graham CH (1997) Effect of transforming growth factor-beta on the plasminogen activator system in cultured first trimester human cytotrophoblasts. *Placenta*, **18**, 137–143.
- Gu Y, Jayatilak PG, Parmer TG, Gauldie J, Fey GH & Gibori G (1992) Alpha 2-macroglobulin expression in the mesometrial decidua and its regulation by decidual luteotropin and prolactin. *Endocrinology*, **13**, 1321–1328.
- Guimond MJ, Luross JA, Wang B, Terhorst C, Danial S & Croy BA (1997) Absence of natural killer cells during murine pregnancy is associated with reproductive compromise in TgE26 mice. *Biol Reprod*, **56**, 169–179.
- Kanayama N, Takahashi K, Matsuura T, Sugimura M, Kobayashi T, Moniwa N, Tomita M & Nakayama K (2002) Deficiency in p57Kip2 expression induces preeclampsia-like symptoms in mice. *Mol Hum Reprod*, **8**, 1129–1135.
- LaMarre J, Wollenberg GK, Gonias SL & Hayes MA (1991) Cytokine binding and clearance properties of proteinase-activated alpha 2-macroglobulins. *Lab Invest*, **65**, 3–14.
- Lorent K, Overbergh L, Delabie J, Van Leuven F & Van den Berghe H (1994) Distribution of mRNA coding for alpha-2-macroglobulin, the murinoglobulins, the alpha-2-macroglobulin receptor and the alpha-2-macroglobulin receptor associated protein during mouse embryogenesis and in adult tissues. *Differentiation*, **55**, 213–223.
- Moffett-King A (2002) Natural killer cells and pregnancy. *Nat Rev Immunol*, **2**, 656–663.
- Overbergh L, Hilliker C, Lorent K, Van Leuven F & Van den Berghe H (1994a) Identification of four genes coding for isoforms of murinoglobulin, the monomeric mouse alpha 2-macroglobulin: characterization of the exons coding for the bait region. *Genomics*, **22**, 530–539.
- Overbergh L, Lorent K, Hilliker C & Van Leuven F (1994b) Characterization of the genes coding for the murinoglobulins and expression in vivo. *Ann N Y Acad Sci*, **737**, 496–497.
- Overbergh L, Lorent K, Torrekens S, Van Leuven F & Van den Berghe H (1995) Expression of mouse alpha-macroglobulins, lipoprotein receptor-related protein, LDL receptor, apolipoprotein E, and lipoprotein lipase in pregnancy. *J Lipid Res*, **36**, 1774–1786.
- Paffaro VA Jr, Bizinotto MC, Joazerio PP & Yamada AT (2003) Subset classification of mouse uterine natural killer cells by DBA lectin reactivity. *Placenta*, **24**, 479–488.
- Peel S (1989) Granulated metrial gland cells. *Adv Anat Embryol Cell Biol*, **115**, 1–112.
- Philip A, Bostedt L, Stigbrand T & O'Connor-McCourt MD (1994) Binding of transforming growth factor-beta (TGF-beta) to pregnancy zone protein (PZP). Comparison to the TGF-beta-alpha 2-macroglobulin interaction. *Eur J Biochem*, **221**, 687–693.
- Sacks GP, Studena K, Sargent IL & Redman CWG (1998) Normal pregnancy and preeclampsia both produce inflammatory changes in peripheral blood leukocytes akin to those of sepsis. *Am J Obstet Gynecol*, **179**, 80–86.
- Sayegh RA, Tao XJ, Leykin L & Isaacson KB (1997) Endometrial alpha-2 macroglobulin; localization by in situ hybridization and effect on mouse embryo development in vitro. *J Clin Endocrinol Metab*, **82**, 4189–4195.
- Sottrup-Jensen L, Stepanik TM, Kristensen T, Wierzbicki DM, Jones CM, Lonblad PB, Magnusson S & Petersen TE (1984) Primary structure of human alpha 2-macroglobulin. V. The complete structure. *J Biol Chem*, **259**, 8318–8327.
- Stewart IJ & Webster AJ (1997) Lectin histochemical studies of mouse granulated metrial gland cells. *Histochem J*, **29**, 885–892.
- Tamada H, McMaster MT, Flanders KC, Andrews GK & Dey SK (1990) Cell type-specific expression of transforming growth factor-beta 1 in the mouse uterus during the periimplantation period. *Mol Endocrinol*, **4**, 965–972.
- Thomas T & Schreiber G (1989) The expression of genes coding for positive acute-phase proteins in the reproductive tract of the female rat. High levels of ceruloplasmin mRNA in the uterus. *FEBS Lett*, **243**, 381–384.
- Umans L, Serneels L, Overbergh L, Stas L & Van Leuven F (1999) alpha2-macroglobulin- and murinoglobulin-1-deficient mice. A mouse model for acute pancreatitis. *Am J Pathol*, **155**, 983–993.
- Van Leuven F. (1982) Human Alpha-2-macroglobulin: structure and function. *TiBS*, **7**, 185–187.
- Yelavarthi KK, Chen HL, Yang YP, Cowley BD Jr, Fishback JL & Hunt JS (1991) Tumor necrosis factor-alpha mRNA and protein in rat uterine and placental cells. *J Immunol*, **146**, 3840–3848.